EMBEDDING OF SUPERELEMENTS FOR THREE-DIMENSIONAL TOPOLOGY OPTIMIZATION

Glaucio H. Paulino
paulino@uiuc.edu
Department of Civil and Environmental Engineering,
University of Illinois at Urbana-Champaign, Newmark Laboratory
205 North Mathews Avenue, Urbana, IL, 61801, U.S.A.
Anderson Pereira
anderson@tecgraf.puc-rio.br
Tecgraf (Group of Technology in Computer Graphics),
Pontifical Catholic University of Rio de Janeiro (PUC–Rio)
Rua Marquês de São Vicente, 225, 22453-900, Rio de Janeiro, RJ, Brazil
Cameron Talischi
ktalisch@uiuc.edu
Department of Civil and Environmental Engineering,
University of Illinois at Urbana-Champaign, Newmark Laboratory
205 North Mathews Avenue, Urbana, IL, 61801, U.S.A.
Ivan F. M. Menezes
Waldemar Celes
ivan@tecgraf.puc-rio.br
celes@tecgraf.puc-rio.br
Tecgraf (Group of Technology in Computer Graphics),
Pontifical Catholic University of Rio de Janeiro (PUC–Rio)
Rua Marquês de São Vicente, 225, 22453-900, Rio de Janeiro, RJ, Brazil

Abstract. *Superelements offer several advantages for high-fidelity solutions of topology optimization problems. Thus this work proposes the use of a two-level mesh representation, involving finite element and topology optimization variables. The proposed mapping–based framework provides a general approach to solve either two-dimensional or three-dimensional problems considering either conventional or non-conventional finite elements.*

Keywords: *Topology optimization, Superelements, Embedding, Mapping*

1. INTRODUCTION

The most common discretization scheme used in topology optimization consists of assigning a constant design variable to each finite element in the domain. The so-called "element-based" approach, however, is known to suffer from numerical instabilities such as the checkerboard phenomenon unless additional restrictions are applied to the design space or higher order finite elements are used (Diaz and Sigmund, 1995; Jog and Haber, 1996). In addition to the accuracy of finite element solutions, the resolution of the final topology is severely limited in this approach. In this work, we examine two-level mesh representation that somehow decouples parameterization of the design field and the finite element discretization of the domain. For a given density mesh, a finer finite element model leads to more stable topology optimization formulation. We will discuss the computational framework for constructing the necessary mapping between the two meshes and present some preliminary results.

2. TWO LEVEL MESH REPRESENTATION

In homogenization-based methods for topology optimization, the design is prescribed by the "density field", which defines the material volume fraction at every point in the extended design domain, see Bendsøe and Sigmund (2003) and the references therein. The response of each candidate design is then used to advance the optimization process. In the case of the structural optimization, the displacement field is used to evaluate the objective function (e.g. compliance) and calculate the gradients (for example, using the adjoint method), based on which the design is updated. Therefore, the resulting topology optimization formulation involves two separate fields, namely the density field and the displacement field. In computational solution schemes, these fields can be discretized independently (Figure 1).

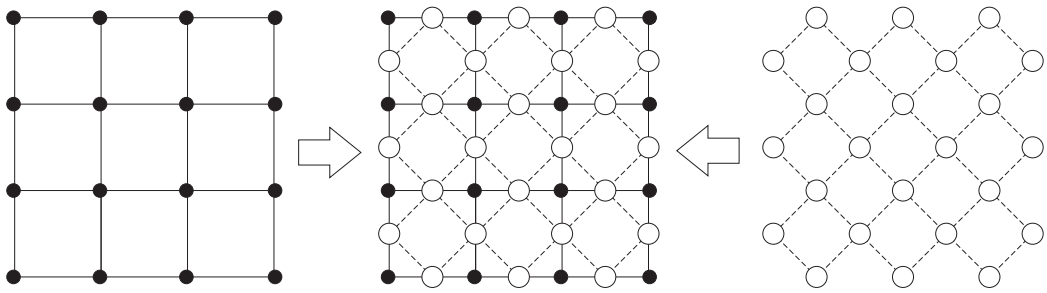

Figure 1: Two level mesh representation. On the far left is the displacement mesh (solid lines), and on the far right is the density mesh (dashed lines). Taken from Paulino and Le (2008).

For the sake of illustration, in this paper, we assume that the finite element mesh is nested inside the density mesh (Figure 2). In other words, the density mesh can be thought of as a subset of the displacement mesh (in a geometric sense). Effectively, this amounts to constructing "superelements" of a group of displacement elements that correspond to the density element. Furthermore, we shall assume that the density is constant inside each element of the density mesh. That is,

$$\rho\left(\mathbf{x}\right) = \sum_{m} \rho_m H_m\left(\mathbf{x}\right) \tag{1}$$

where H_m is the Heaviside function with the support limited to density (material) element m:

$$H_m\left(\mathbf{x}\right) = \begin{cases} 0, & \mathbf{x} \notin \Omega_m \\ 1, & \mathbf{x} \in \Omega_m \end{cases} \tag{2}$$

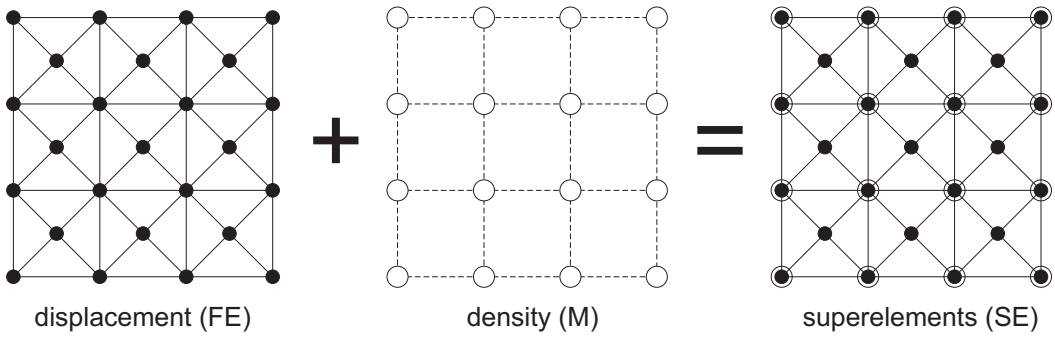

Figure 2: Illustration of the case where the displacement mesh is nested inside the density mesh.

For this parameterization ρ_m is the set of design variables for the optimization problem. Note that the piecewise discretization of the density field is not the only choice. It is also possible to choose the density at the nodal locations as the design variables and interpolate the density elsewhere using finite element shape functions. This approach is referred to as the Continuous Approximation of Material Distribution (CAMD) and is studied in Matsui and Terada (2004). With the CAMD approach, we no longer need to require that the displacement mesh is nested inside the density mesh as the density field is C^0 continuous throughout the domain.

3. TOPOLOGY OPTIMIZATION PROBLEM

For this work, we consider benchmark compliance minimization problem, in which the objective is to find the stiffest structures composed of a fixed volume of material subjected to a set of loads and supports. In the discrete setting, we have:

$$\begin{aligned} \min_{\rho,\mathbf{u}} \quad & c(\rho,\mathbf{u}) = \mathbf{f}^T\mathbf{u} \\ \text{s.t.:} \quad & \mathbf{K}(\rho)\mathbf{u} = \mathbf{f} \\ & V(\rho) = \int_{\Omega_s} \rho dV \leq V_s \end{aligned} \tag{3}$$

Here, $\mathbf{f}$ and $\mathbf{u}$ are the global load and displacement vectors, $\mathbf{K}$ is the global stiffness matrix, and V_s is the prescribed upper bound on the volume of the structure. Note that the dependence of stiffness matrix on ρ is based on the relation between the volume fraction of a point and its stiffness. Here, we use the popular Solid Isotropic Material with Penalization (SIMP) model, see Bendsøe and Sigmund (2003) for example, which defines the constitutive matrix as:

$$\mathbf{C}(\mathbf{x}) = [\rho(\mathbf{x})]^p \mathbf{C}^0, \quad p > 1 \tag{4}$$

where $\mathbf{C}^0$ is the constitutive matrix for the solid phase, corresponding to $\rho = 1$. To avoid the singularity of the stiffness matrix, a small positive lower bound is placed on the density:

$$0 < \rho_{min} \leq \rho \leq 1 \tag{5}$$

For our numerical implementation, we used a continuation on the value of the exponent p, by gradually increasing its value from $p = 1$ to $p = 4$ by 0.5. This alleviates the problem of converging to local minima.
The sensitivity of the objective function and volume constraint with respect to the design variable ρ_m can be calculated as follows:

$$\frac{\partial c}{\partial \rho_m} = \mathbf{u}^T \frac{\partial \mathbf{K}}{\partial \rho_m} \mathbf{u}, \qquad \frac{\partial V}{\partial \rho_m} = \int_{\Omega_m} \rho dV \equiv V_s \tag{6}$$

To construct the stiffness matrix and compute the gradient $\partial \mathbf{K}/\partial \rho_m$, we need a mapping that connects the two meshes. This is discussed in more detail in the next section. With the sensitivities computed, we solve the optimization problem using the Method of Moving Asymptotes (MMA), developed in Svanberg (1987).

4. MAPPING BETWEEN TWO DISCRETIZATIONS

Consider the finite element FE in the displacement mesh. The stiffness matrix for this element is given by:

$$\mathbf{K}_{FE} = \int_{\Omega_{FE}} \mathbf{B}^T \mathbf{C} \mathbf{B} dV = \int_{\Omega_{FE}} \left[\sum_i \rho_i H_i(\mathbf{x}) \right]^p \mathbf{B}^T \mathbf{C}^0 \mathbf{B} dV \tag{7}$$

If FE is nested inside density element m, then:

$$\mathbf{K}_{FE} = (\rho_m)^p \mathbf{K}^0_{FE} \tag{8}$$

where $\mathbf{K}^0_{FE} = \int_{\Omega_{FE}} \mathbf{B}^T \mathbf{C}^0 \mathbf{B} dV$ is the stiffness matrix for the reference element. The collection of finite elements that lie in the support of density element m can be defined as $\mathcal{S}_m$:

$$\mathcal{S}_m = \{FE : \Omega_{FE} \subseteq \Omega_m\} \tag{9}$$

With this definition, the sensitivity of the compliance can be localized:

$$\frac{\partial c}{\partial \rho_m} = -\sum_{FE \in \mathcal{S}_m} \left[\mathbf{u}^T_{FE} \frac{\partial \mathbf{K}_{FE}}{\partial \rho_m} \mathbf{u}_{FE} \right] = -\sum_{FE \in \mathcal{S}_m} \left[p(\rho_m)^{p-1} \mathbf{u}^T_{FE} \mathbf{K}^0_{FE} \mathbf{u}_{FE} \right] \tag{10}$$

The task of determining the collection $\mathcal{S}_m$ is strictly geometric, which must be carried out using the two input meshes for density and displacement.

5. NUMERICAL RESULTS

In general, two independent interpolations to approximate the displacement field and the material density field are used in the solution of topology optimization. The conventional solution when implemented with the element–based approach is denoted as $\square/U$, where $\square$ is the element whose displacement field will be approximated, and U refers to uniform material density inside each element. In this work, our mapping approach is implemented by splitting the density mesh in order to approximate the displacement field and it is denoted as $\square/SE$. Figure 3 shows the notation used in this work.

We have applied the mapping approach for two problems: the benchmark MBB beam problem for the two-dimensional case and a three-dimensional cantilever problem.

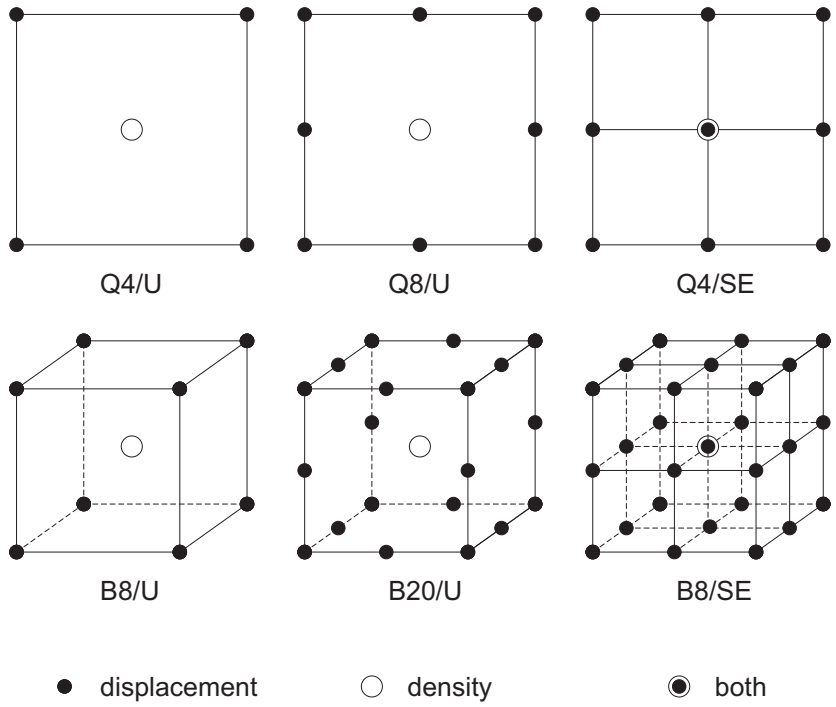

Figure 3: Mapping between displacement and density meshes used in this paper.

5.1 $2D$ MBB Problem

The so–called MBB beam is illustrated by Figure 4. The density mesh for this problem is uniform and made up of square elements. The displacement mesh is constructed such that four $Q4$ elements are contained inside each density element, named $Q4/SE$. Results are compared with the element-based approach using uniform $Q4$ and $Q8$ elements, named $Q4/U$ and $Q8/U$, respectively, see Figure 3.

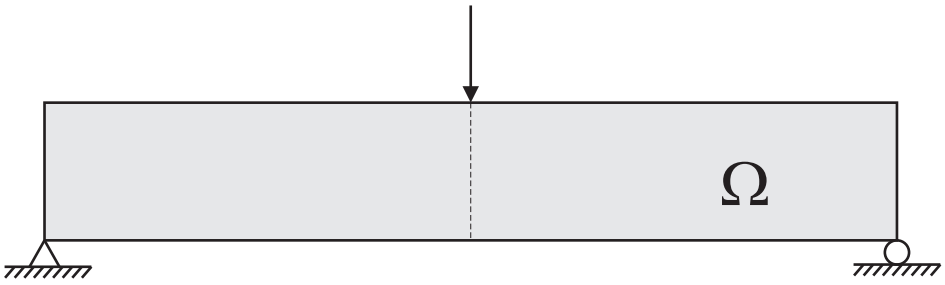

Figure 4: Schematic representation of the design domain, loading and boundary conditions for MBB (Messerschmitt-Bölkow-Blohm) beam problem.

The results obtained are show in Figure 5. As expected, the $Q4/U$ results exhibit the checkerboard patterns, while the $Q8/U$ results don't. The "superelement" ($Q4/SE$) results are also checkerboard–free and follow the expected Michell–type patterns. Note that due to the geometry of the density discretization, one-node hinges may still appear even though the checkerboard problem is removed. A plot of the compliance versus number of iterations is provided in Figure 5(d). Table 1 shows the final values of the optimization solution.

(a) 90×30 $Q4/U$

(b) 90×30 $Q8/U$

(c) 180×60 $Q4/SE$

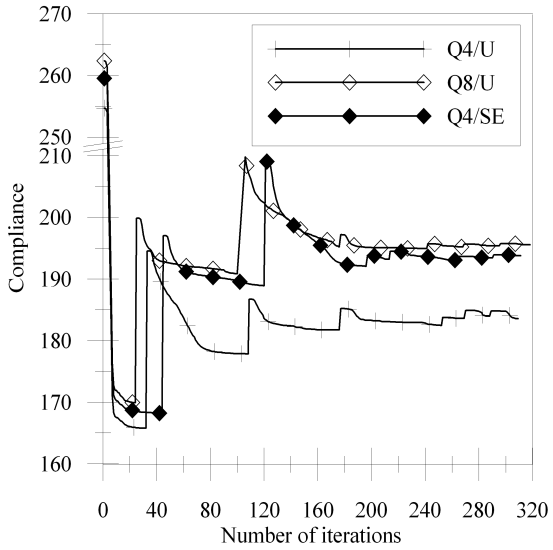

(d) Convergence history for the objective function (compliance) for the MBB beam problem.

Figure 5: Results for the MBB beam problem.

Table 1: Final results for the MBB beam problem.

Mapping	Number of iterations	Compliance
$Q4/U$	309	183.6
$Q8/U$	318	195.6
$Q4/SE$	311	193.8

5.2 $3D$ Cantilever problem

The $3D$ cantilever beam studied in this paper is illustrated by Figure 6. Analogous to the $2D$ problem, the density mesh in this case is uniform and made up of hexahedral elements. The displacement mesh is constructed such that eight $B8$ elements are contained inside each density element ($B8/SE$), see Figure 3. Results are compared to the element-based approach using uniform $B8$ and $B20$ elements ($B8/U$ and $B20/U$), see Figure 7. The $B8$ results exhibit the $3D$ checkerboard patterns, while the $B20$ results are free from these anomalies. Table 2 shows the final values of the optimization solution while a plot of the compliance versus number of iterations is provided in Figure 7(d).

Table 2: Final results for the $3D$ Cantilever problem.

Mapping	Number of iterations	Compliance
$B8/U$	210	365.0
$B20/U$	191	403.7
$B8/SE$	269	420.4

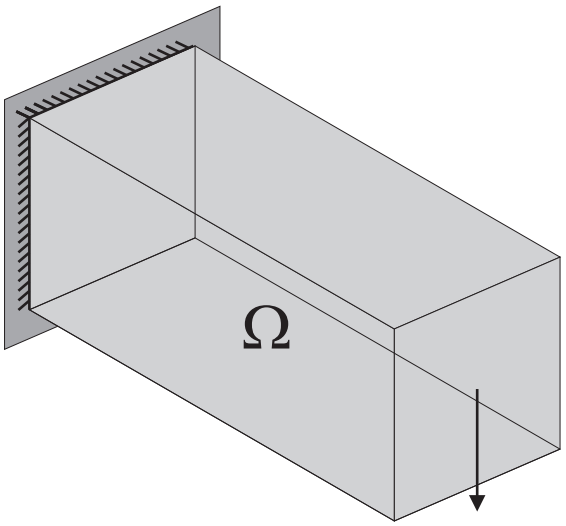

Figure 6: Schematic representation of the design domain, loading and boundary conditions for cantilever beam problem.

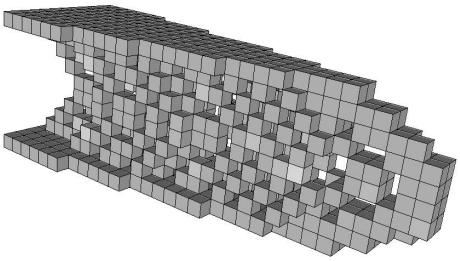

(a) $30 \times 10 \times 10$ $B8/U$

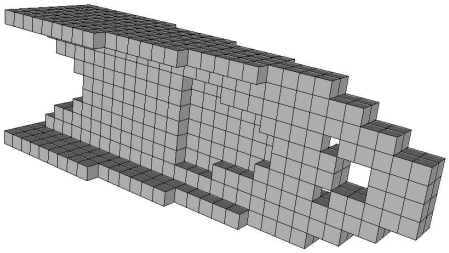

(b) $30 \times 10 \times 10$ $B20/U$

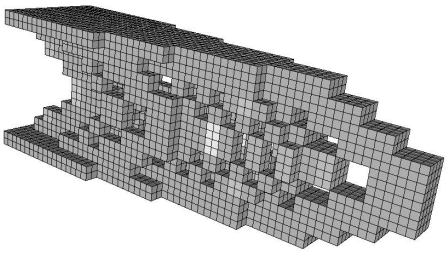

(c) $60 \times 20 \times 20$ $B8/SE$

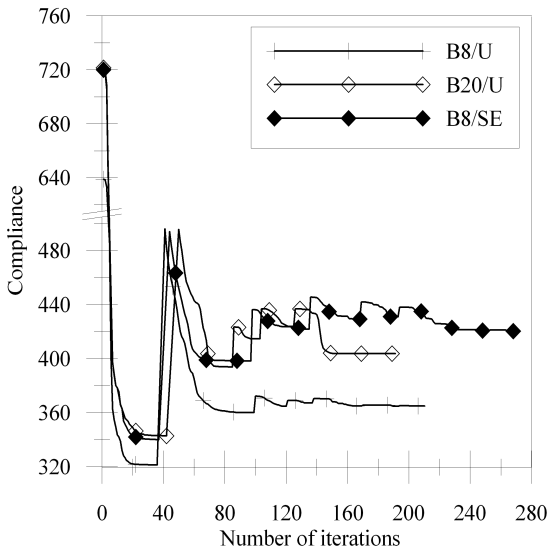

(d) Convergence history for the objective function (compliance) for the $3D$ Cantilever problem.

Figure 7: Results for the $3D$ Cantilever problem.

6. CONCLUSIONS AND EXTENSIONS

The mesh embedding proposed in this paper is a promising technique for high fidelity topology optimization. The finite element mesh is nested inside the density mesh. In other words, the density mesh can be thought of as a subset of the displacement mesh (in a geometric sense). Effectively, this amounts to constructing "superelements" of a group of displacement elements that correspond to the density element. Future work includes the application of the method to non-coincident meshes, two-level mesh representation using topological data structure, and independent adaptivity capabilities for the two meshes.

ACKNOWLEDGEMENTS

The authors Cameron Talischi and Glaucio Paulino acknowledge the support by the Department of Energy Computational Science Graduate Fellowship Program of the Office of Science and National Nuclear Security Administration in the Department of Energy under contract DE-FG02-97ER25308. We are grateful to Prof. Krister Svanberg (Svanberg, 1987) for providing the MMA (Method of Moving Asymptotes) code, which was used to generate the examples in this paper. Anderson Pereira, Ivan Menezes and Waldemar Celes acknowledge the financial support provided by Tecgraf (Group of Technology in Computer Graphics), PUC-Rio, Rio de Janeiro, Brazil.

REFERENCES

Bendsøe, M. & Sigmund, O., 2003. *Topology Optimization–Theory, Methods and Applications*. Berlin: Springer.

Diaz, A. & Sigmund, O., 1995. Checkerboard patterns in layout optimization. *Structural Optimization*, vol. 10, pp. 40–45.

Jog, C. S. & Haber, R. B., 1996. Stability of finite element models for distributed-parameter optimization and topology design. *Computer Methods in Applied Mechanics and Engineering*, vol. 130, pp. 203–226.

Matsui, K. & Terada, K., 2004. Continuous approximation of material distribution for topology optimization. *International Journal for Numerical Methods in Engineering*, vol. 59, pp. 1925–1944.

Paulino, G. H. & Le, C., 2008. A modified Q4/Q4 element for topology optmization. *Structural and Multidisciplinary Optimization*. In press.

Svanberg, K., 1987. The method of moving asymptotes – A new method for structural optimization. *International Journal for Numerical Methods in Engineering*, vol. 24, pp. 359–373.